

# Copper Oxide Thin Films by Successive Ionic Layer Adsorption and Reaction (SILAR): A Sustainable Approach for Solar-Driven Methylene Blue (MB) Degradation

Yugen Kulkarni<sup>1,2</sup>, Niketa Pawar<sup>1,2</sup>, Namrata Erandole<sup>1</sup>, Muskan Mulani<sup>1</sup>, Mujjammil Shikalgar<sup>1</sup>, Swapnil Banne<sup>2</sup>, Dipali Potdar<sup>2</sup>, Ravindra Mane<sup>2</sup>, Smita Mahajan<sup>2</sup>, Prashant Chikode<sup>2,\*</sup>

\*prashantchikode@gmail.com

<sup>1</sup> Department of Physics, Willingdon College, Sangli, 416415, India

<sup>2</sup> Department of Physics, Jaysingpur College, Jaysingpur, 416101, India

Received: December 2023

Revised: March 2024

Accepted: March 2024

DOI: 10.22068/ijmse.3539

**Abstract:** The paper investigates the solar photodegradation of Methylene Blue dye using copper oxide (CuO) thin films synthesized by the Successive Ionic Layer Adsorption and Reaction (SILAR) method. The structural, morphological, and optical characteristics of the CuO thin films have been investigated by employing a variety of methods, such as Fourier transform Infrared (FTIR) spectroscopy, UV-Vis spectroscopy, Scanning electron microscopy (SEM), and X-ray diffraction (XRD). The outcomes showed that CuO thin films with excellent surface shape and a highly crystalline nature had been successfully deposited. Methylene Blue was subjected to solar radiation during its photodegradation process, and the outcomes showed a significant decrease in the dye's concentration over time. To maximize the photodegradation process, the effects of other experimental factors were also assessed, such as the starting concentration of MB, the quantity of CuO thin film, the number of SILAR cycles and the pH of the solution. Good photocatalytic activity is demonstrated by CuO thin films produced using the SILAR approach in the solar photodegradation of methylene blue. The development of affordable and ecologically friendly wastewater treatment technology that can use sun energy to break down persistent organic contaminants is affected by these findings.

**Keywords:** Photo-catalysis, Wastewater treatment, CuO, Methylene Blue, Solar energy.

## 1. INTRODUCTION

Water pollution remains a pressing global environmental concern and it is getting worse due to diverse anthropogenic activities. Among the numerous sources of contamination, the discharge of industrial effluents containing synthetic dyes significantly contributes to the deterioration of water quality. Dyes, extensively used in textile, leather, paper, and other industries, pose a substantial threat due to their persistence, toxicity and resistance to conventional wastewater treatment methods [1-3]. One such dye of considerable environmental consequence is Methylene Blue (MB), a cationic thiazine dye extensively employed in various industrial processes [1, 4]. The International Union of Pure and Applied Chemistry (IUPAC) gives it the chemical name [7-(dimethylamino) phenothiazin-3-ylidene] - dimethylazanium; chloride (Fig 1). Despite its use as a dye, it also is widely used in various fields like textile, paper, paint, food and even medical fields [1-5]. It is considered a safe drug for therapeutic treatments with a concentration of less than 2 mg/kg [5]. But it can be present at higher

concentrations in the wastewater.

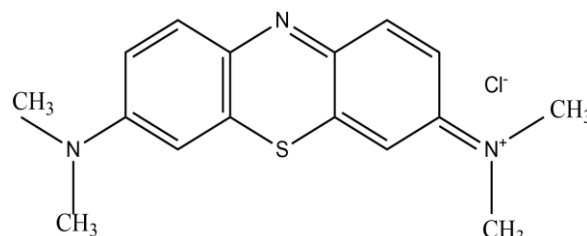
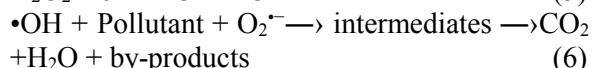
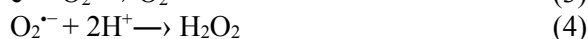
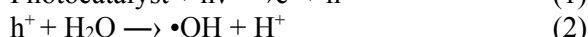
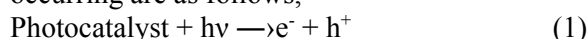


**Fig. 1.** Chemical Structure of Methylene Blue (MB).

Methylene Blue, with its prominent use as a textile dye, poses a considerable risk to aquatic ecosystems due to its resistance to biodegradation and potential adverse health effects. The need for effective and sustainable remediation strategies to combat dye-induced water pollution has driven researchers to explore advanced oxidation processes (AOPs), such as photocatalysis, as promising methods for dye degradation. Photocatalysis, utilizing semiconductor materials to harness solar or artificial light for the degradation of organic pollutants, has emerged as an environmentally benign approach [2, 6-9]. As shown in Fig. 2, the mechanism of

photocatalysis involves the activation of a semiconductor photocatalyst, typically metal oxides, by exposure to light with energy greater than or equal to their bandgap. This excitation generates electron-hole pairs, creating reactive oxygen species (ROS) such as hydroxyl radicals ( $\cdot\text{OH}$ ) and superoxide radicals ( $\text{O}_2^{\cdot-}$ ) [10-12].

These highly reactive species then engage in redox reactions with the organic dye molecules, leading to their degradation into simpler and less harmful by-products. The series of reactions occurring are as follows,



Copper oxide (CuO) thin films, synthesized through methods like Successive Ionic Layer Adsorption and Reaction (SILAR), have gained attention as efficient photocatalysts for dye degradation.

The unique properties of CuO, including its band gap structure, non-toxicity, high chemical stability and photocatalytic activity, make it a compelling candidate for sustainable and effective water treatment. It is a p-type material with a direct band gap of around 1.2 eV-1.8 eV. This indicates that it is

photosensitive to visible light and makes solar-driven photocatalysis significant [13 -14].

## 2. EXPERIMENTAL PROCEDURES

### 2.1. Synthesis of CuO by SILAR Method

CuO thin films on glass substrates are prepared with the SILAR method (Fig. 3).

AR grade reagents were used without further purification. The mixture of Copper sulphate pentahydrate ( $\text{CuSO}_4 \cdot 5\text{H}_2\text{O}$ ) and sodium thiosulphate ( $\text{Na}_2\text{S}_2\text{O}_3$ ) is used as a cationic precursor (beaker A). Sodium hydroxide (NaOH) was used as an anionic precursor (beaker C).

The cationic precursor was kept at room temperature, while the anionic precursor was kept at a constant temperature of  $70^\circ\text{C}$ . The successive SILAR cycles were carried out at 25, 45, 60, and 80 cycles and optimized at 60 cycles. Prepared thin films were dried at room temperature and annealed at  $120^\circ\text{C}$  for 1 hour to remove hydrates and to reduce hydroxide to oxide.

### 2.2. Photodegradation of MB

A solution of 5 ppm MB dye is prepared in water. The degradation of MB is observed under dark and sunlight with and without the presence of CuO films. Conditions like pH and temperature are kept identical for both cases. The active area of each CuO film was about  $1200 \text{ mm}^2$ .

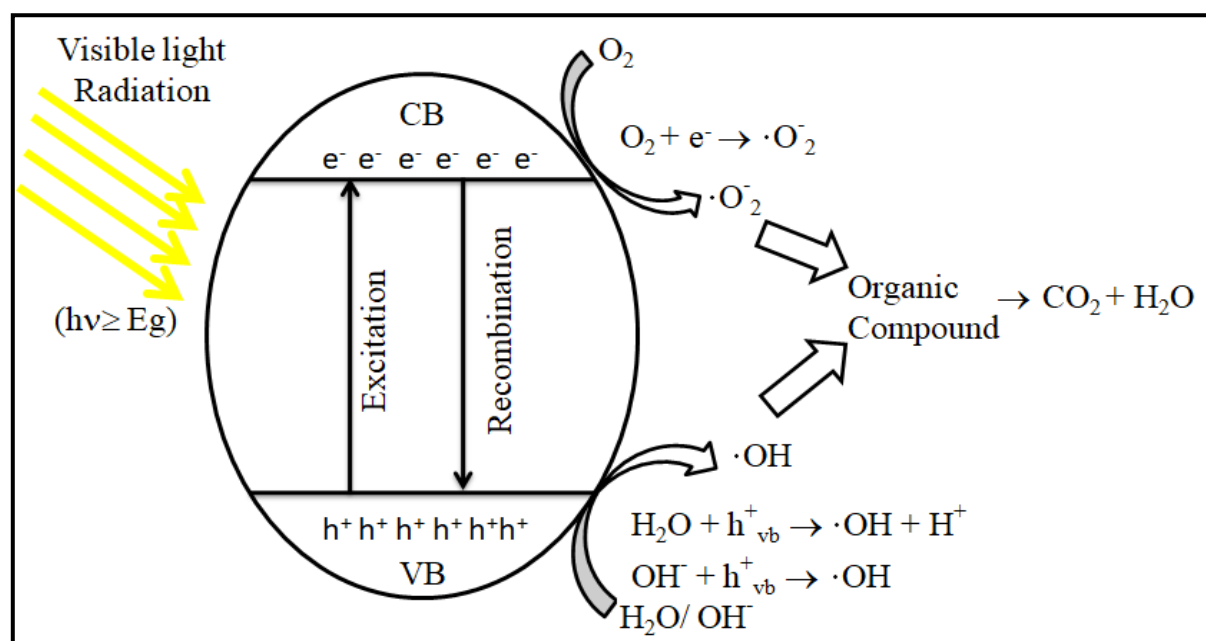


Fig. 2. Mechanism of photocatalysis using semiconductor for degradation of organic compounds.

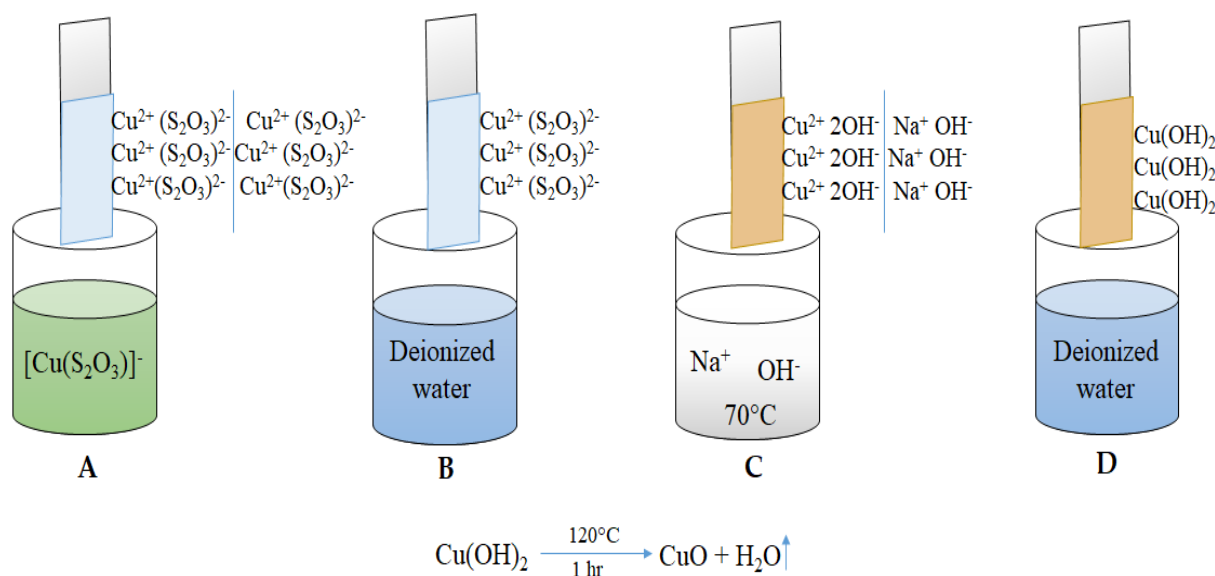


Fig. 3. Schematic representation of the deposited CuO thin films by SILAR method.

The samples were collected after intervals of every 15 minutes up to 90 minutes to check the degradation using UV-visible spectroscopy.

After completion of these series, the effect of pH on the rate of degradation is checked by adding ammonia (for basic pH) and hydrochloric acid (HCl) (for acidic pH). At the end effect of hydrogen peroxide (H<sub>2</sub>O<sub>2</sub>) is also studied.

### 3. RESULTS AND DISCUSSION

The deposited films were characterized by different characterization techniques. X-ray diffraction study (XRD) was done for the structural analysis.

Ultraviolet-visible (UV-Vis) and Fourier Transform Infrared (FTIR) spectroscopy were done for bandgap energy calculations and functional group detection, respectively. Scanning Electron Microscopy (SEM) and Energy Dispersive X-ray Analysis (EDX) were used to study the morphology and elemental configuration of prepared thin films. Apart from that, contact angle measurements were also done.

#### 3.1. X-ray Diffraction (XRD)

X-ray diffraction (XRD) spectroscopy of the sample was made with the help of Cu-K $\alpha$  wavelength (1.5406 Å). Figure 4 shows the XRD pattern after deposition of 60 cycles.

CuO was confirmed using Profex (open source) software and JCPDS no. 00-002-1041. The peaks of CuO are observed at 34.01°, 35.91°, 40.00°, 53.39° representing (111), (022), (202), and (113)

planes respectively. (022) and (202) planes showed maximum intensity. Two peaks were observed at lower angles (16.67° and 23.88°) and the noise is due to the glass (SiO<sub>2</sub>) substrate. The nature of the graph shows the polycrystalline nature of CuO.

Broader peaks represent smaller crystallite sizes. The crystallite size was calculated using the Debye-Scherer formula,

$$D = \frac{k \lambda}{\beta \cos \theta}$$

Where k is shape factor = 0.9

$\lambda = 0.154 \text{ nm} = \text{Cu-K}\alpha$  wavelength used for XRD analysis  $\beta$  is Full width at half maxima (FWHM).

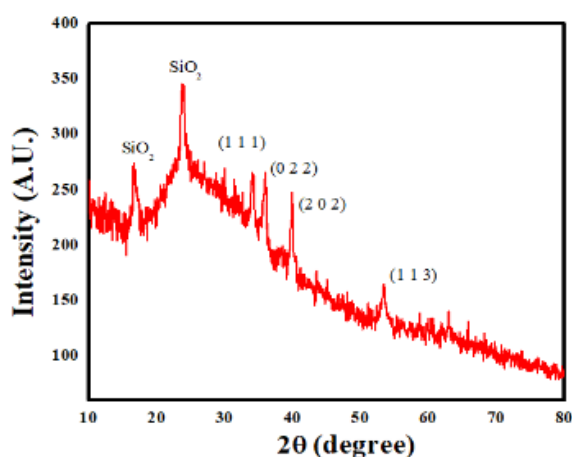


Fig. 4. XRD pattern of CuO thin films.

The minimum crystallite size is about 2 nm and the maximum is 4.92 nm. The average crystallite size is found to be 3.36 nm.

### 3.2. UV-Vis Spectroscopy

UV-Vis spectroscopy was done to find the bandgap of the material. Fig. 5 shows the absorbance vs wavelength graph. The data is analyzed using the Tauc's equation,

$$\alpha h\nu = A (h\nu - E_g)^n$$

Where,

$$\alpha \text{ is the absorption coefficient} = \frac{2.303 \times \text{absorbance}}{\text{thickness}}$$

$E_g$  is bandgap

$h\nu$  is the energy of the photon

$A$  is constant

$n = 0.5$  gives allowed indirect transition (indirect bandgap)

$n = 2$  gives allowed direct transition (direct bandgap)

The thickness of the film for 60 SILAR cycles is found 2.19  $\mu\text{m}$ . Tauc's plot (Fig. 6) shows the direct bandgap of the film is about 1.45 eV.

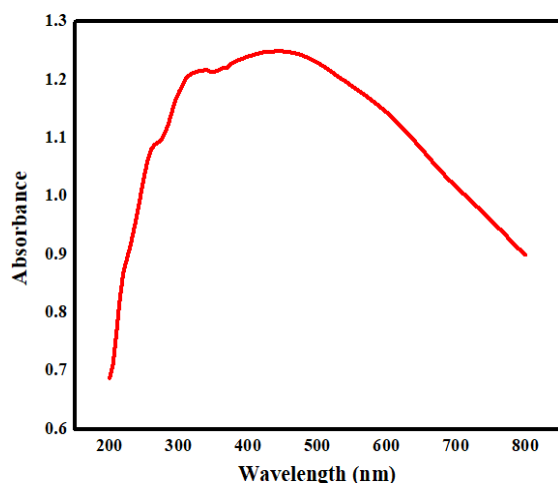


Fig. 5. UV- Visible absorption spectra of CuO thin films

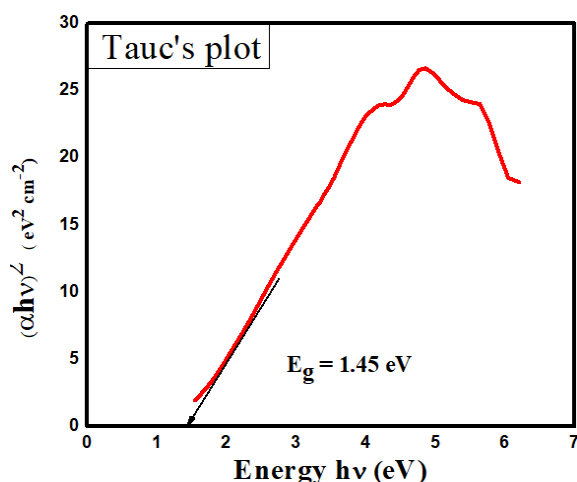


Fig. 6. Tauc's Plot for CuO thin film

### 3.3. Fourier Transform Infrared (FTIR) Spectroscopy

Absorption peaks at 534  $\text{cm}^{-1}$ , 618  $\text{cm}^{-1}$  and 779  $\text{cm}^{-1}$  confirm CuO material (Fig. 7). The peaks at 1024  $\text{cm}^{-1}$ , 1109  $\text{cm}^{-1}$  and 1538  $\text{cm}^{-1}$  represent O-H bending, while the peaks at 1641  $\text{cm}^{-1}$  and 3449  $\text{cm}^{-1}$  show O-H stretching vibrations.

The presence of the OH group is because of the water molecules from air adsorbed on the material. As the material moves into the nano-region, its surface-to-volume ratio increases which leads to more water adsorption on the surface [15].

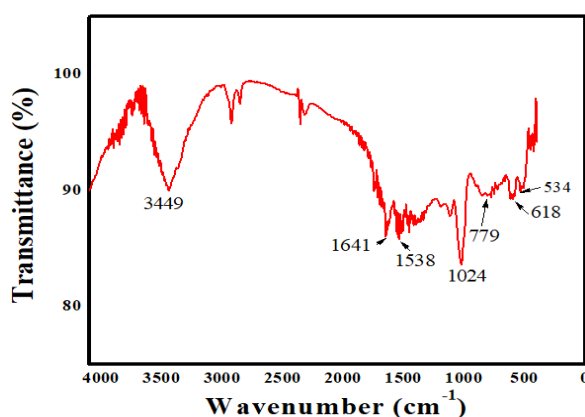


Fig. 7. FTIR pattern of CuO thin film.

### 3.4. Scanning Electron Microscopy with Electron Dispersive X-Ray Analysis

Scanning Electron Microscopy (SEM) was used to analyze the surface morphology of CuO thin films. SEM images of various magnifications are shown in Fig. 8. At a magnification of  $\times 500$ , it shows agglomerated structures and at a magnification of  $\times 10000$ , it reveals a cascade fibre-like structure. The average grain size of the grains is in the range of 520 nm-530 nm. The chemical composition of the prepared material was identified by Electron Dispersive X-ray (EDX) analysis. Fig. 9 shows the EDX spectra of CuO thin films, which confirms the presence of copper and oxygen. The peak of Silicon (Si) is due to the glass ( $\text{SiO}_2$ ) substrate. Atomic and mass concentration (in %) of Cu, O and Si in films were obtained from EDX analysis and the results are as shown in Table 1. Atomic and mass concentration reveals the presence of CuO along with  $\text{SiO}_2$ .

### 3.5. Contact angle Measurement

Using a C-T meter, the contact angle between CuO

film and tap water is measured. The average angle obtained is  $36.9^\circ$ . As the contact angle is acute, it is evident that CuO film is hydrophilic. The film does get wet with water implying good adsorption of water and hence better dye degradation.

### 3.6. Photocatalytic Activity of CuO

CuO films were used to degrade the Methylene Blue (MB) dye. Initially, photodegradation of only MB dye is observed under the sunlight. It is observed that a 1 ppm solution of dye can be

degraded completely within 2 hours in the absence of any photocatalyst. As per the literature, the concentration of MB below 2 ppm is not hazardous at all, it is used in medical applications [5]. Therefore, in this work, we focused on the degradation of 5 ppm dye under various conditions. The UV-Vis spectroscopy of MB shows a characteristic peak at 664 nm (Fig. 11). The decrease in intensity represents the degradation of the dye. It is also evident from the decolorization of MB (Fig. 10).

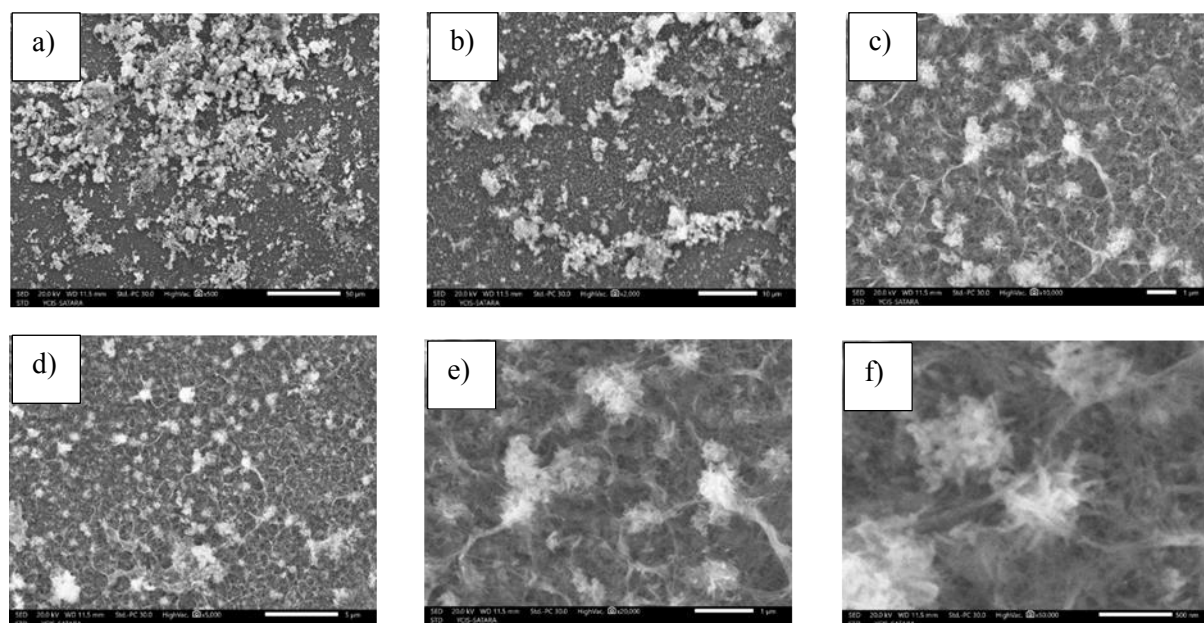


**Fig. 8.** Scanning Electron Micrographs of CuO thin films with a magnification of a)  $\times 500$ , b)  $\times 2000$ , c)  $\times 5000$ , d)  $\times 10000$ , e)  $\times 20000$  and f)  $\times 50000$ .

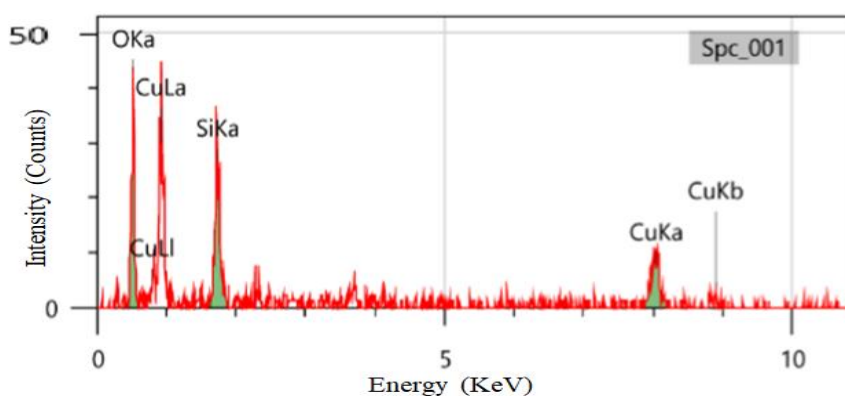


**Fig. 9.** Energy Dispersive X-ray (EDX) spectrum of CuO thin film.

**Table 1.** Mass and atomic concentration (%) of various elements in CuO thin films.

Elements	Mass Concentration %	Atomic Concentration %
O	$36.55 \pm 2.45$	$62.43 \pm 4.18$
Cu	$44.48 \pm 4.79$	$19.13 \pm 2.06$
Si	$18.96 \pm 1.84$	$18.45 \pm 1.79$
<b>Total</b>	<b>100</b>	<b>100</b>

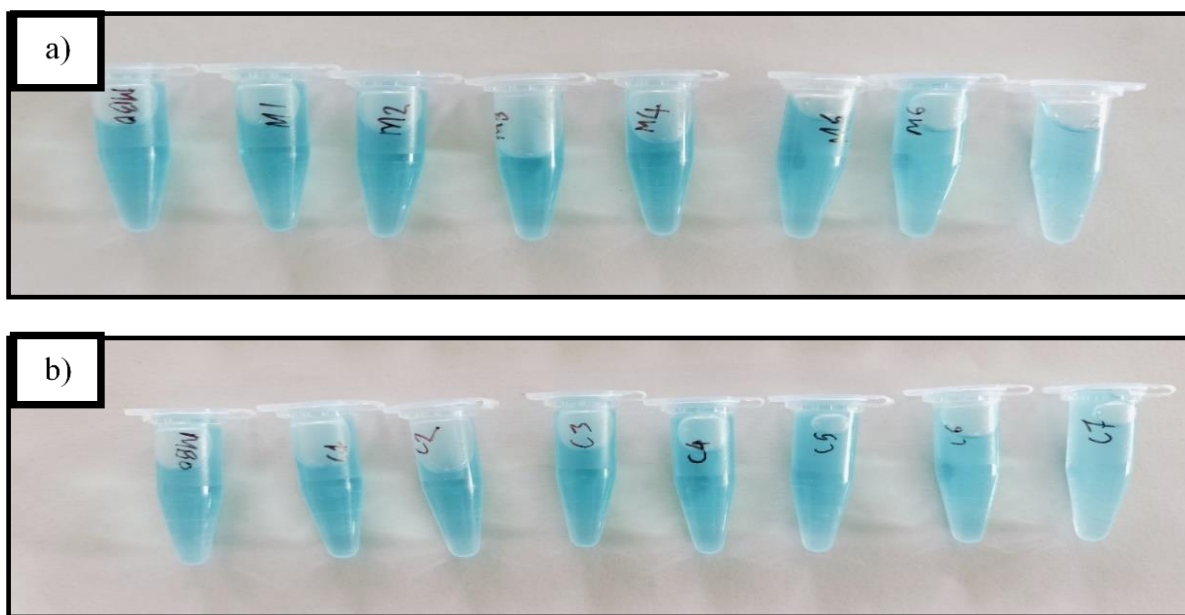


**Fig. 10.** Decolorization of Methylene Blue after every 15 minutes in sunlight in the a) absence of CuO films and b) presence of CuO films.

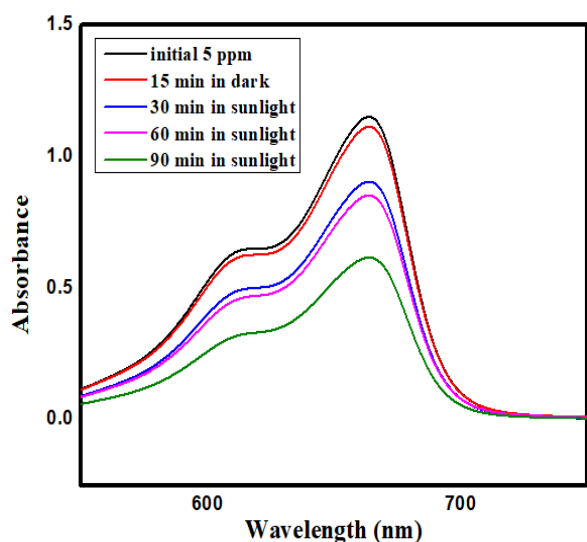


**Fig. 11.** UV-Visible spectra for degradation of MB under sunlight without CuO films.

A dye without photocatalyst showed 46.44 % degradation in 90 minutes (Fig. 11), while the presence of CuO films increased the degradation percentage up to 51.15% within the same duration (Fig. 12). CuO film provides both degradation and adsorption and hence faster decolorization as shown in Fig. 13.

In the initial stage (up to 30 min.), degradation of MB in the absence of CuO film seems to have higher degradation than that of in the presence of CuO films, due to adsorption. As time progresses, the degradation of MB in the presence of CuO

becomes faster as adsorption is completed (Fig. 14). Adding Hydrogen peroxide ( $H_2O_2$ ) to the dye solution increases the rate of degradation in the presence of sunlight. But further increase in the concentration of  $H_2O_2$  reduces the rate of degradation. It is also observed that the rate of degradation in the presence of both CuO films and  $H_2O_2$  is very high. Hence the optimum concentration needs to be found.

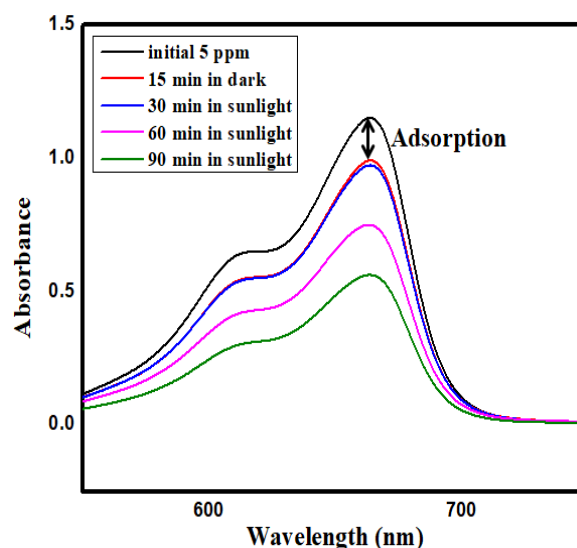


**Fig. 12.** UV-Visible spectra for degradation of MB under sunlight with CuO films.

We have varied concentrations (Table 2) and found 1 ml  $H_2O_2$  in 100 ml dye solution (10 ml/L)

degrades the dye completely in 40 minutes and it is the optimized concentration.  $H_2O_2$  can improve the concentration of hydroxyl ions and hence the degradation becomes very fast. But if the concentration goes beyond a certain optimum value, the intensity of photons reaching the photocatalyst and dye may also reduce hence lowering the rate of degradation.

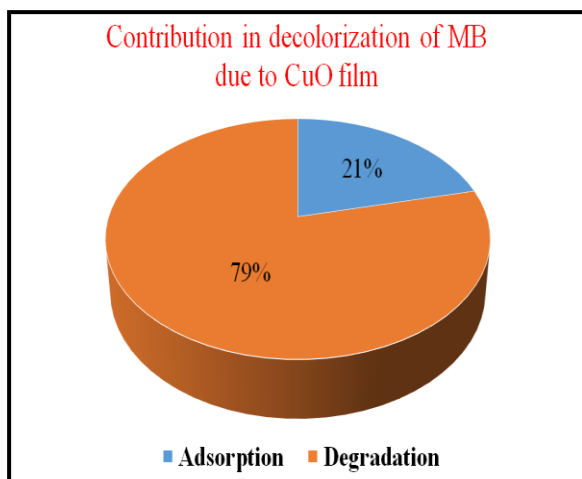


**Fig. 13.** Contribution of adsorption and degradation in decolorization of MB.

**Table 2.** Effect of addition of  $H_2O_2$  in dye solution during degradation.

Concentration of $H_2O_2$ (ml/L)	Time taken for complete degradation (min.)
5	45
10	40
15	50

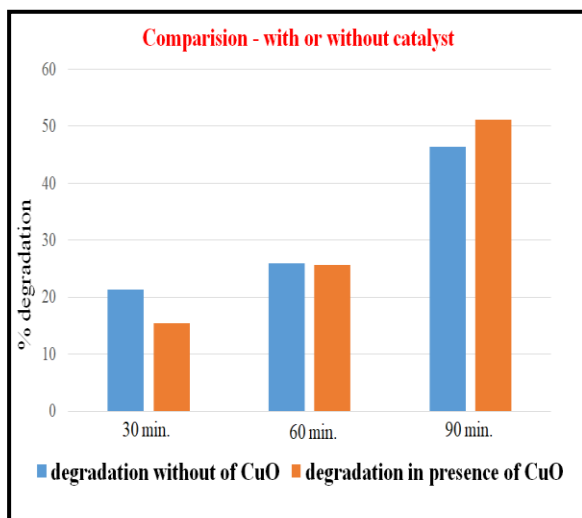


**Fig. 14.** Comparison of degradation with and without CuO films.

Variation in pH may seem to improve the degradation of dye. At basic pH conditions (pH=11), UV-Vis analysis shows reduced absorbance in the visible range at the characteristic peak (664 nm) and increased absorbance at other wavelengths. Despite reduced absorbance at the characteristics peak, samples were not much decolorized (Fig. 15). In fact, after keeping the sample for a while, a blue precipitate (ppt) was formed at the bottom of the container. This suggests that MB is not degraded but separated from the wastewater. These particles of MB can then be collected easily using filtration or centrifugation. At acidic conditions, a dye cannot degrade by itself and the CuO film also becomes useless as it dissolves in acidic media. Prepared films were used multiple times for the degradation of MB. No deterioration in photocatalytic activity was found, denoting very high reusability of prepared CuO films.

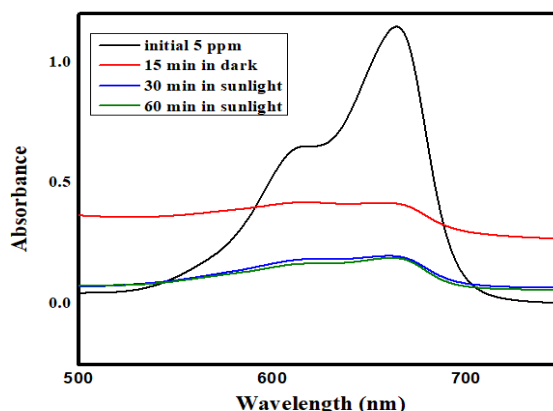


**Fig. 15.** UV-visible spectra for degradation of MB under sunlight at pH= 11.

#### 4. CONCLUSIONS

CuO films prepared using the SILAR method exhibited excellent photocatalytic activity toward methylene blue dye. It is found that a dye at low concentrations (eg. 1 ppm) can get photo-degraded even in the absence of catalysts. However, at higher concentrations, the catalyst is needed to speed up the degradation. It is also observed that the presence of  $H_2O_2$  at optimized conditions improves the rate of degradation. Variation in pH affects the process in such a way that at basic pH conditions, the adsorption of MB on the catalyst surface increases and the dye can get precipitated from the dissolved state which then can be easily separated.

## CONFLICTS OF INTEREST

There are no conflicts to declare including any competing financial interest.

## ACKNOWLEDGEMENTS

The authors are thankful to the DST-FIST laboratory, Jaysingpur College, Jaysingpur for characterization as well as Willingdon College, Sangli for making the laboratory and facilities available. They are also thankful to the Common Facility Center (CFC), Shivaji University, Kolhapur for providing an XRD facility.

## REFERENCES

- [1]. Sarkar Phyllis, A. K., Tortora, G. & Johnson, I. Photodegradation. Fairchild Books Dict. Text. (2022) doi:10.5040/9781501365072.12105.
- [2]. Shanker, U., Rani, M. & Jassal, V. Degradation of hazardous organic dyes in water by nanomaterials. *Environ. Chem. Lett.* (2017)15, 623–642.
- [3]. Sharma, J., Sharma, S. & Soni, V. Classification and impact of synthetic textile dyes on Aquatic Flora: A review. *Reg. Stud. Mar. Sci.* (2021) 45,101802.
- [4]. Din, M. I., Khalid, R., Najeeb, J. & Hussain, Z. Fundamentals and photocatalysis of methylene blue dye using various nanocatalytic assemblies- a critical review. *J. Clean. Prod.* (2021) 298, 126567.
- [5]. Prashant R. Ginimuge, J. S. D. Methylene Blue: Revisited. *Clin. Pharmacol.* (2010) 26, 517–520.
- [6]. Shindhal, T., Rakholiya ,P., Varjani, S., Pandey, A., Ngo, HH., Guo ,W. , Ng, HY., Taherzadeh, MJ., A critical review on advances in the practices and perspectives for the treatment of dye industry wastewater. *Bioengineered* (2021)12, 70–87.
- [7]. Sharma, K., Dalai, A. K. & Vyas, R. K. Removal of synthetic dyes from multicomponent industrial wastewaters. *Rev. Chem. Eng.* (2017) 34, 107–134.
- [8]. Makertihartha, I. G. B. N., Rizki, Z., Zunita, M. & Dharmawijaya, P. T. Dyes removal from textile wastewater using graphene-based nanofiltration. *AIP Conf. Proc.* (2017) 1840,110006. doi: 10.1063/1.4982336.
- [9]. Pedanekar, R.S., Madake S.B., Narewadikar, N.A., Mohite, S.V., Patil, A.R., Kumbhar, S.M., Rajpure, K.Y., Photoelectrocatalytic degradation of Rhodamine B by spray deposited Bi<sub>2</sub>WO<sub>6</sub> photoelectrode under solar radiation. *Mater. Res. Bull.* (2022)147, 111639.
- [10]. Mudhoo, A., Paliya, S., Goswami, P., Singh, M., Lofrano, G., Carotenuto, M., Carraturo, F., Libralato, G., Guida, M., Usman, M. & Kumar, S., Fabrication, functionalization and performance of doped photocatalysts for dye degradation and mineralization: a review. *Environmental Chemistry Letters*, (2020) 18, 1825-1903.
- [11]. Anwer, H., Mahmood, A., Lee, J., Kim, K.H., Park, J.W., Yip, A.C.K., Photocatalysts for degradation of dyes in industrial effluents: Opportunities and challenges. *Nano Res.* (2019)12, 955–972.
- [12]. Kamble, R., Sabale, S., Chikode, P., Puri, V. & Mahajan, S. Structural and photocatalytic studies of hydrothermally synthesized Mn<sup>2+</sup>-TiO<sub>2</sub> nanoparticles under UV and visible light irradiation. *Mater. Res. Express*, (2016) 3, 1–10.
- [13]. Kumar, R., Murugadoss, M., Pirogov, G., & Thangamuthu R., A facile one-step synthesis of SnO<sub>2</sub>/CuO and CuO/SnO<sub>2</sub> nanocomposites: photocatalytic application. *J. Mater. Sci. Mater. Electron.* (2018) 29, 13508–13515.
- [14]. Bayat, F. & Sheibani, S. Enhancement of photocatalytic activity of CuO-Cu<sub>2</sub>O heterostructures through the controlled content of Cu<sub>2</sub>O. *Mater. Res. Bull.* (2022)145, 111561.
- [15]. Varughese, A., Kaur, R. & Singh, P. Green Synthesis and Characterization of Copper Oxide Nanoparticles Using Psidium guajava Leaf Extract. *IOP Conf. Ser. Mater. Sci. Eng.* (2020) 961, 012011, doi:10.1088/1757-899X/961/1/012011.